JOURNAL OF EXPERIMENTAL AND THEORETICAL PHYSICS, 2024, Vol. 165, No. 5, pp. 662–671

SOLIDS AND LIQUIDS

LOCAL STRUCTURE AND SOLIDIFICATION OF GLASSFORMING MELT $AL_{86}NI_6CO_4GD_2TB_2$ UNDER HIGH PRESSURE: EXPERIMENT, MODELING, MACHINE LEARNING

© 2024 S. G. Menshikova [a,*], N. M. Shchelkachev [b,**]

[a] Udmurt Federal Research Center
of the Ural Branch of the Russian Academy of Sciences
426067, Izhevsk, Russia
[b] Vereshchagin Institute for High Pressure Physics
of the Russian Academy of Sciences
142190, Moscow, Troitsk, Russia
* e-mail: svetlmensh@udman.ru
** e-mail: n.chtchelkatchev@gmail.com

Received October 27, 2023
Revised January 09, 2024
Accepted January 09, 2024

Abstract. High pressure affects melt solidification and its glass-forming ability. Ab initio molecular dynamics calculations show how the local structure of the melt changes with increasing pressure. High pressure promotes the formation of icosahedral clusters in the melt. Rare earth elements: gadolinium, terbium facilitate the formation of icosahedra. At a pressure of 10 GPa and melt temperature of 1800 K, icosahedra atoms form a "percolation cluster". As pressure decreases, the concentration of icosahedra decreases, and at atmospheric pressure, icosahedra are practically absent. Thus, the glass-forming ability of the melt increases with increasing pressure. Using deep machine learning techniques, the dependence of glass transition temperature on high pressure was evaluated: pressure increase from 0 to 10 GPa increases by 1.3 times. The structure of solid alloy samples obtained by cooling its melt from 1800 K at a rate of 1000 degrees/s under 10 GPa pressure was studied. X-ray diffraction and electron microscopy methods showed that the samples are dense and homogeneous, with a fine-dispersed structure. New crystalline phases with cubic (c$P4$ / 2) and tetragonal ($tI26$ / 1) structures, stable for long periods under normal conditions, were synthesized in the alloy. Rare earth elements play a major role in the formation of the phase with cubic structur (c$P4$ / 2). Studies showed that the average hardness of samples obtained at 10 GPa is almost 2 times higher than that of the initial sample obtained at atmospheric pressure, and is about 2 GPa.

DOI: 10.31857/S004445102405e055

1. INTRODUCTION

Progress in understanding the processes occurring in high-temperature glass-forming melts of Al-TM-REM type (TM – transition metal, REM – rare earth metal) with aluminum content of 80-90 at.% in a wide temperature range [1,2], as well as in studying the effects of high pressures and cooling rates on their solidification [3] has high scientific significance. At cooling rates of 100,000 degrees/s, alloys vitrify forming ribbons with a thickness of about 50-60 μm. There is interest in increasing the glass-forming ability of melts of this type of system. There is reason to believe that extreme impacts (EI) (high pressures, temperatures, and cooling rates) can help in solving this issue. Development of methods for obtaining alloys under such extreme conditions is a complex technological challenge. Under conditions of high pressures and temperatures during high-speed solidification of the melt, physical and chemical processes occur that are difficult or in some cases impossible under normal conditions due to thermodynamic limitations. EI affects both the

kinetics and thermodynamics of melt solidification. In particular, high pressure increases the viscosity of the metallic melt and also modifies the short-range order structure towards denser packings, including non-crystalline ones. Besides the general tendency towards grain refinement, EI promotes crystallization of new metastable phases, usually denser ones. As a result, materials with unique structures and properties can be obtained [3-8].

The rapid development of computer technologies makes it possible to conduct theoretical studies of realistic systems using various methods, particularly within the *ab initio* (AIMD) [9][1] approach. Recently, *ab initio* calculation methods based on density functional theory (DFT)[2] have become increasingly widespread in the study of condensed matter physics, which is also of high interest for studying alloys of the above-mentioned system [10].

Of great interest is also the use of artificial neural networks (ANN) (deep machine learning) [11, 12] in quantum mechanics, in correlated systems, and in systems with phase transitions. "Deep" denotes the degree of complexity (depth) of the neural network, which can often be quite superficial. Neural network training is a process in which neural network parameters are adjusted through modeling the environment in which the network is embedded. The type of training is determined by the method of parameter adjustment. The main disadvantage of ANN is the need to obtain large experimental data for network training, as well as low predictive ability. Advantages include: the ability to achieve high calculation accuracy, and also, when there are no physical models of structural or other dependencies – simplicity of training and use when necessary experimental data and software are available [13]. Using ANN, it is possible to build models for calculating yield strength and strain hardening of industrial aluminum alloys based on structural parameters [13], predicting shortrange ordering behavior in binary and multicomponent aluminum-based alloys, depending on concentration and temperature [14]. Recently, it was discovered that crystal nucleation in supercooled melt reaches maximum speed at the glass transition temperature and significantly slows down during deep cooling in the glassy state [15].

Previously, we conducted experimental and theoretical studies of solidification of a fourcomponent glass-forming melt $Al_{86}Ni_2Co_6Gd_6$ under high pressure [16]. We discovered new metastable phases forming in the alloy after thermobaric treatment of the melt during solidification. We showed that the glass-forming ability of the melt increases with increasing high pressure. Similar studies are practically absent in literature. The purpose of this work is to study the local structure of the melt at low and high pressures in a more complex glassforming alloy $Al_{86}Ni_6Co_4Gd_2Tb_2$; to investigate the effect of high pressure on melt solidification and its glass-forming ability.

2. MATERIALS AND RESEARCH METHODS

2.1. Experiment

The ingot of specified composition was obtained by melting pure metals in corundum crucibles in a Tammann furnace. The following elements were used as initial components with the main metal content: aluminum 99.999, nickel 99.9, cobalt 99.9, gadolinium 99.9, terbium 99.9 (wt.%). Chemical analysis of the ingot showed that the content of main elements corresponded to the specified composition within ±0.2% from nominal. The obtained sample was considered as initial. Samples for high-pressure studies at 10 GPa were obtained in a "toroid" type chamber [17]. Heating and melting of the sample were carried out by passing alternating current through it. Alget stone was used as the pressure-transmitting medium. Experimental procedure: pressure establishment → pulse heating → holding at established pressure and temperature → cooling without pressure release to room temperature → reduction of high pressure to atmospheric. The cooling rate of melts was 1000 degrees/s, melt temperature before quenching was 1800 K. Phase composition of samples was determined by X-ray diffraction analysis. Electron microscopy methods were used to study the elemental composition, morphology, and size

[1] A first-principles calculation method describing atomic interactions taking into account quantum effects.

[2] A method for calculating the electronic structure of many-particle systems in quantum physics and quantum chemistry.

of structural constituents of the alloy. Hardness measurements H_V were performed on a PMT-3M hardness tester. Load applied to the indenter ~ 50 g, loading time ~ 10 s. Values H_V were averaged over 20 measurements.

2.2. Modeling

Structural studies of the melt were performed using density functional theory based on VASP (The Vienna Ab initio Simulation Package). Elementary cells of 512 atoms with periodic boundary conditions were considered at the Gamma point. The plane wave basis cutoff energy was 500 eV. Due to low concentrations of Ni, Co, Gd and Tb, the modeling was performed using 10 independent melt replicas with different initial random atom positions. Random initial configurations were created based on hard-sphere interaction potential between atoms and classical (LAMMPS) molecular dynamics modeling. The most disordered configurations were selected using the USPEKH algorithm. Equilibrium configuration was achieved through VASP modeling of the system in NPT ensemble for at least 10 ps with a 1 fs step. Then the systems were modeled using VASP in NVT ensemble in Nose-Hoover thermostat at high temperatures and pressures. To study the melt during deep undercooling, a machine learning interaction potential (MLIP) was constructed using quantum molecular dynamics data as a training dataset. The DEEPMD package was used[3] as the kernel for MLIP assembly. "se_a" descriptors with 7 Å cutoff were selected for processing training data. The initial training database for MLIP machine learning was obtained by random sampling of 20% quantum molecular dynamics data, while the remaining 80% quantum molecular dynamics data, while the remaining data was used in the validation dataset. Multi-stage MLIP potential refinement was performed using the DPGEN (Deep Potential GENerator) package, which at each stage evaluates the accuracy of classical molecular dynamics by calculating the dispersion of interatomic forces across an ensemble of four MLIP replicas and

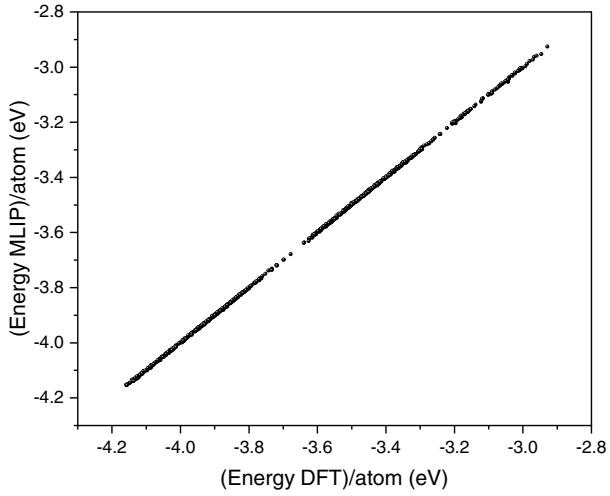

Fig. 1. Comparison of forces calculated using MLIP and DFT

sends the least accurate configurations for DFT VASP calculation with their subsequent addition to the training database. The process converges when the dispersion of interatomic forces becomes less than the specified threshold for 90% configurations generated by DPGEN. Since some atoms in the alloy have very low concentrations, it became necessary to add a small number of high-entropy configurations to the training database, where concentrations of all elements are of the same order. This is necessary to stabilize the convergence of the MLIP learning procedure in the case of alloyed systems, where alloying elements, due to low concentration, rarely come close together. As a result, the accuracy of MLIP, compared to the initial calculation, was

Energy MAE/Natoms	$1.808373 \cdot 10^{-3}$ eV,
Energy RMSE/Natoms	$1.103514 \cdot 10^{-1}$ eV,
Force MAE	$2.263140 \cdot 10^{-03}$ eV/A,
Force RMSE	$1.570985e-01$ eV/A,
Virial MAE/Natoms	$9.203836 \cdot 10^{-03}$ eV,
Virial RMSE/Natoms	$1.190558 \cdot 10^{-23}$ eV.

Here, MAE denotes the Mean Absolute Error, and RMSE stands for Root Mean Square Error compared to DFT. The deviation of MLIP calculations from DFT is graphically shown in Fig. 1 and Fig. 2. Classical molecular dynamics (CMD) with MLIP has accuracy comparable to quantum molecular dynamics. The most important thing is that CMD can handle a sufficiently large number of particles and propagate them over 10 μs

[3] DEEPMD is designed to minimize the effort required to build a deep learning-based model of interatomic potential energy and force field, as well as to perform classical molecular dynamics (CMD) calculations.

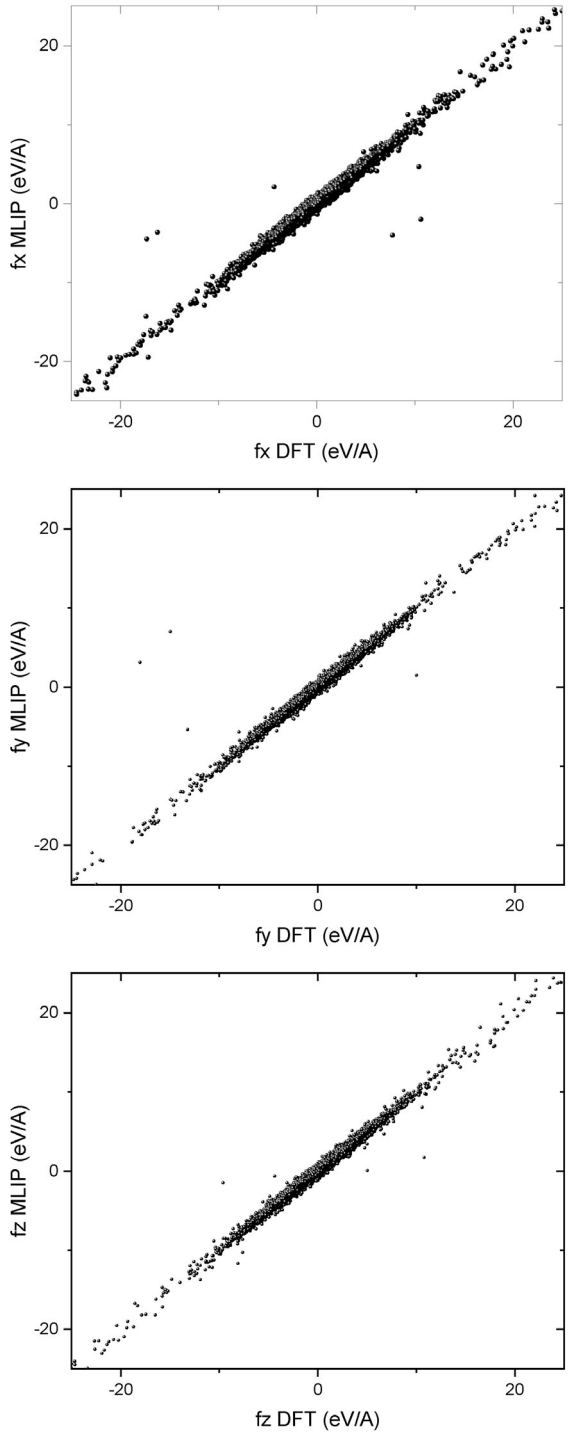

Fig. 2. Comparison of forces calculated using MLIP and DFT

time periods rather than 1–10 ns. We chose LAMMPS for CMD. For CMD melt simulation, we selected a cell with 13824 atoms under periodic boundary conditions and a time step of 2 fs. The alloy was simulated during cooling using the Nose-Hoover NPT thermostat from 2000 to 100 K for 10 million MD steps.

3. RESULTS AND DISCUSSION

3.1. Experiment

Previously, alloy samples $Al_{86}Ni_6Co_4Gd_2Tb_2$, were studied depending on high pressure (up to 10 GPa) and melt quenching temperature (up to 1800 K) [18]. It was shown that at pressures of 7–10 GPa, new metastable phases form in the alloy: phase $(Al_3Gd))^*$ (of type Al_3U), with primitive cubic structure (with ($cP4/2$) and phase $(Al_8(Co/Ni)_4(Gd))^*$ (of type Al_8Cr_4Gd) with tetragonal structure ($tI26/1$). Studies performed in this work showed that in the alloy $Al_{86}Ni_6Co_4Gd_2Tb_2$, under the same conditions, phases of the same composition are formed (see table), however, the structure morphology is different. Rare earth metals, in our case, Gd and Tb, show great similarity in chemical and physical properties, which is explained by almost identical structure of outer electronic levels of their atoms, have approximately equal atomic radii and are easily interchangeable in the studied alloy. Thus, the formation of the same phases in the alloy $Al_{86}Ni_6Co_4Gd_2Tb_2$ as in the alloy $Al_{86}Ni_2Co_6Gd_6$ is quite justified. Fig. 3*a* shows the microstructure of the alloy sample $Al_{86}Ni_6Co_4Gd_2Tb_2$, obtained in a Tammann furnace by melting pure components at atmospheric pressure and a sample obtained under pressure of 10 GPa (Fig. 3*b*). The quenching temperature in both cases was 1800 K. Fig. 3 shows that the structure of the sample obtained under 10 GPa pressure is more dispersed compared to the sample obtained at normal atmospheric pressure. Studies have also shown that the sample obtained under high pressure is homogeneous, dense, without shrinkage cavities and pores; the average microhardness is almost twice as high as in the initial sample, and is about 2 GPa. The discovered new phases form in alloys at high pressures of 7-10 GPa. At pressures less than 7 GPa, only equilibrium phases are present in the alloy.

3.2. Modeling

As a result of modeling melts at 1800 K and pressures of 0 and 10 GPa, radial distribution functions of atoms (RDF) were obtained and studied. Fig. 4 shows the total RDFs. When pressure increased to 10 GPa, an increase in peaks and their shift was noted, which indicates an increase in the degree of local ordering in the melt at high pressure. Analysis of partial RDFs of the melt

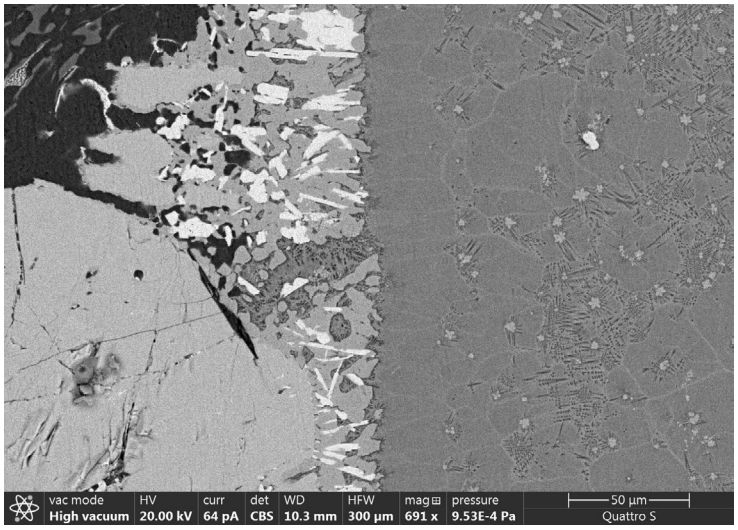

a *b*

Fig. 3. Microstructure of alloy samples $Al_{86}Ni_6Co_4Gd_2Tb_2$, obtained in a Tammann furnace by melting pure components at atmospheric pressure (a) and obtained under pressure of 10 GPa (b) ((1800 K, 1000 deg/s)

Table. Conditions of obtaining and phase composition of alloy samples $Al_{86}Ni_6Co_4Gd_2Tb_2$

No.	Obtaining conditions	Phase composition
1	atm. pressure (1800 K)	α-Al; Al_3Gd (hex., $hP8$ / 3); $Al_{19}Ni_5(Tb/Gd)_3$(orth., $oC108$ / 4)
2	10 GPa (1800 K)	α-Al, Al_3(Gd/Tb)*(Ni/Co) (of type Al_3Er) (cub., $cP4$ / 2),
		$Al_8(Co/Ni)_4$(Gd/Tb)** (of type Al_8Cr_4Gd) (tetr., $tI26$ / 1)

at 0 and 10 GPa (1800 K) for aluminum, cobalt, nickel, gadolinium, and terbium showed that high pressure mainly affects the local environment of aluminum, gadolinium, and terbium in the melt. A similar situation was noted by us earlier for the alloy $Al_{86}Ni_2Co_6Gd_6$ [16], where high pressure primarily affects the local environment of aluminum and gadolinium in the melt.

For the analysis of short-range order in atomic arrangements, a method known as "polyhedral template matching" [19] was used. Based on the PRDF, the maximum bond length was selected as 3Å. As a parameter controlling the determination of local symmetry, RMSD (Root Mean Square Deviation)[4] equal to 1.1 was chosen. Analysis of molecular dynamics trajectories showed that at zero pressure in the melt $Al_{86}Ni_6Co_4Gd_2Tb_2$ in small concentration (0.5%), icosahedral clusters are present (Fig. 5*a*). When pressure increases to 10 GPa, their concentration increases to at least (Fig. 5*b*). In this calculation of icosahedra concentration, only atoms having the nearest icosahedral environment were considered, i.e., at the center of the icosahedron. The division of icosahedral matter into clusters in the melt is also

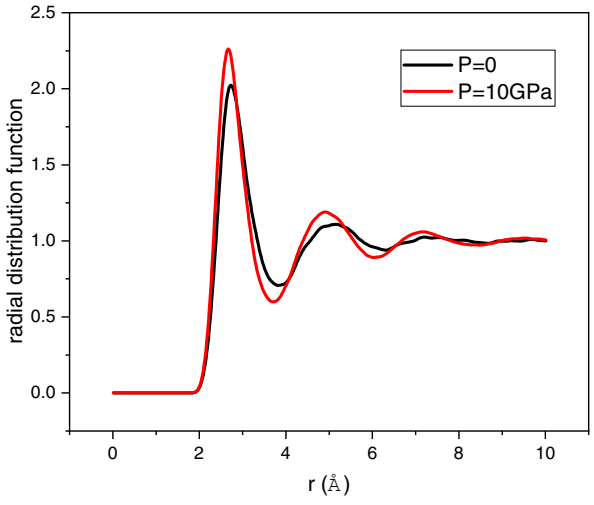

Fig. 4. Total PRDF of the melt $Al_{86}Ni_6Co_4Gd_2Tb_2$ (1800 K)

[4] A measure of the average distance between atoms.

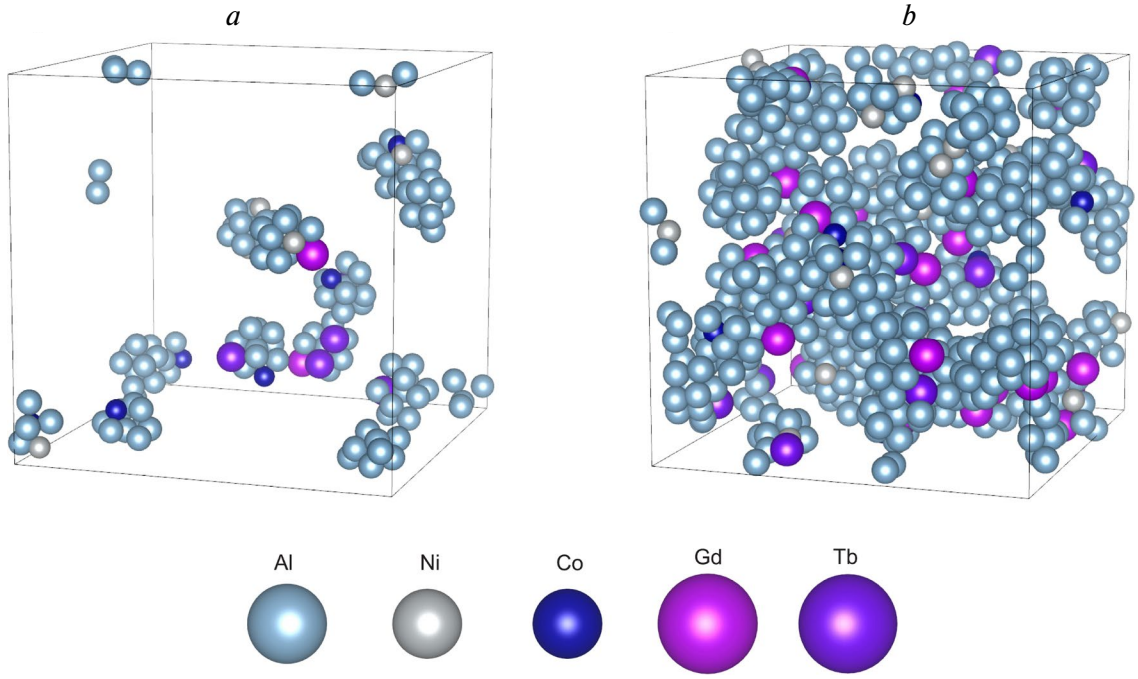

Fig. 5. Icosahedral clusters in the melt $Al_{86}Ni_6Co_4Gd_2Tb_2$ at 0 (a) and 10 (b) GPa (1800 K)

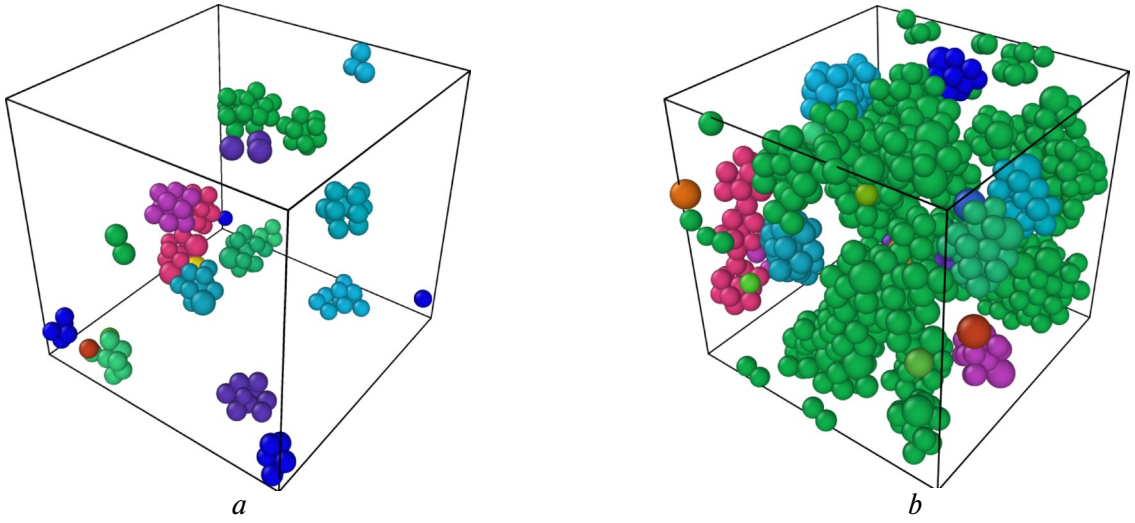

Fig. 6. Division of icosahedral matter into clusters in the melt $Al_{86}Ni_6Co_4Gd_2Tb_2$ at 0 (a) and 10 (b) (1800 K)

shown in Fig. 6 *a,b*. Atoms belonging to one cluster are united by one color. The green color shows the "network" of icosahedra – the "percolation cluster"[5]. That is, at 10 GPa, atoms form a "percolation cluster," while at atmospheric pressure, they do not. For both pressures, calculations were performed at 1800 K. If at zero pressure the systems are cooled by 200 K, from 1800 to 1600 K, after pressure reduction from 10 to 0 GPa, the concentration of icosahedra decreases. The network of icosahedra in metallic liquid is usually an indicator of its glass-forming ability. Thus, it can be assumed that with increasing pressure, the glass-forming ability of the melt also increases.

Figure 7*a* shows the percentage ratio of atoms at the centers of icosahedra to the total number of atoms at 10 GPa pressure in the temperature range from 2000

[5] A cluster that has a path from the upper to the lower boundary of the considered area.

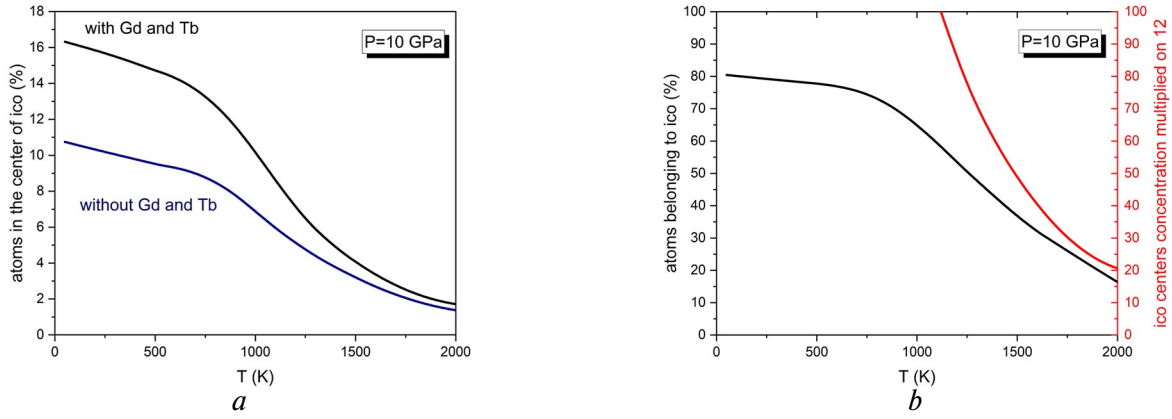

Fig. 7. Number of atoms at the centers of icosahedra (a) and belonging to icosahedra (b), relative to the total number of atoms (%)

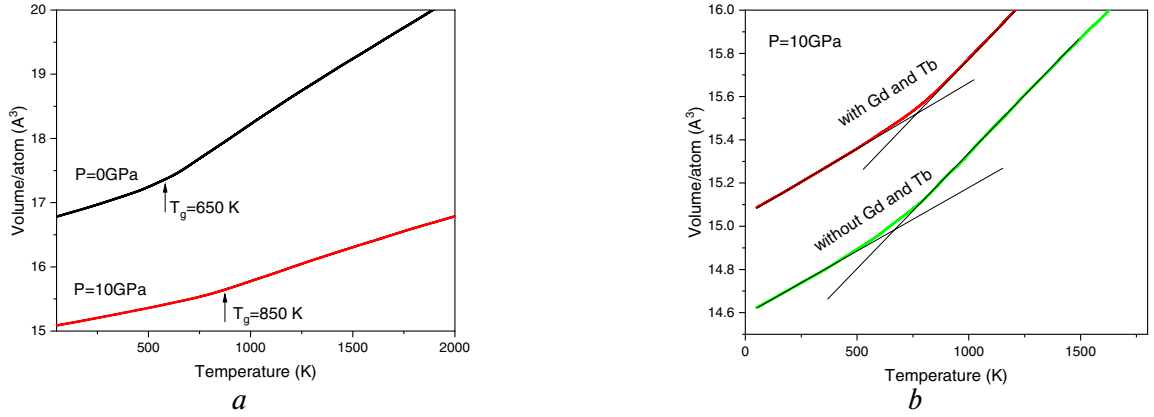

Fig. 8. Temperature dependence of the alloy volume $Al_{86}Ni_6Co_4Gd_2Tb_2$ per atom at pressures of 0 and 10 GPa (a), the same dependence at 10 GPa in the absence of Gd and Tb (b)

to 0 K. Two cases are considered: with rare earth metals (REM) present in the melt (black curve) and without REM (blue curve). Fig. 7*a* shows that at high temperatures this percentage is practically identical for both curves, while at lower temperatures there is a significant difference. Fig. 7*b* shows the percentage change with temperature of the number of atoms belonging to icosahedra. Further theoretical studies showed that the alloy without REM amorphizes in a film-like manner, while with REM present – in bulk form. In several works, particularly in [20, 21], it is shown that some single-component extremely cooled metal melts are characterized by the presence of icosahedral short-range order. Usually, icosahedral clusters in such melts, for example, in aluminum melt, are absent at high temperatures or their quantity is insignificantly different from zero [15].

It is known that, as in second-order phase transitions, glass formation is accompanied by a sharp change in heat capacity and thermal expansion coefficient [22-24]. In this case, a kink is observed in the temperature dependence of volume. We estimated the dependence of glass transition temperature on pressure based on the temperature dependence of volume per atom. Using atomistic computer simulation of cooling a melt of 5000 atoms, with MLIP, the glass transition temperature was determined (T_g): about 650 K at normal pressure and 850 K at 10 GPa pressure for the alloy $Al_{86}Ni_6Co_4Gd_2Tb_2$ (Fig. 8*a*). For the alloy $Al_{86}Ni_2Co_6Gd_6$: about 600 K at normal pressure and about 820 K at 10 GPa pressure [16]. The obtained glass transition temperatures constitute 0.5 of their melting temperature, which agrees well with literature data for similar metallic systems [25]. We estimated how much T_g of alloy $Al_{86}Ni_6Co_4Gd_2Tb_2$, changes if REMs are removed from the alloy. The removal of Tb and Gd leads to a decrease in T_g by approximately 65 K (Fig. 8*b*).

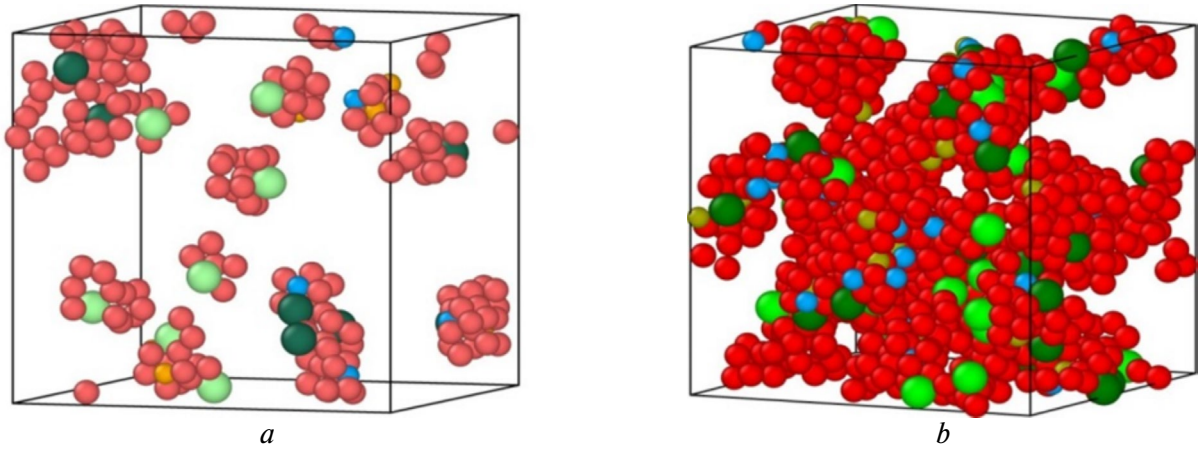

Fig. 9. Icosahedra in the bulk of supercooled melt at temperature 500 K, below T_g. Aluminum atoms are highlighted in red, nickel atoms in blue, cobalt atoms in yellow (a) and brown (b), gadolinium atoms in light green, terbium atoms in dark green

Thus, external conditions and the state of the melt affect its solidification. This must be taken into account when developing technological processes for obtaining materials with specified properties. It is known that melt crystallization occurs through the formation of crystalline nuclei that develop into crystals. Spontaneously arising crystallization centers (nuclei) lead to a decrease in volumetric free energy and an increase in interfacial energy due to the interface. For the formation of crystal nuclei in a liquid, certain conditions are necessary, in particular, the appearance of microvolumes where the mutual arrangement of atoms would correspond to the crystal lattice of the forming solid alloy. In the studied melt at atmospheric pressure and temperature of 1800 K, a small number of icosahedral clusters were found, whose concentration increases with pressure. In icosahedral clusters, it is important to know how atoms are arranged in space. Icosahedral clusters under external conditions (temperature, pressure, etc.) can rearrange and change to increase density and occupied volume, as this is energetically favorable [26]. The relative size of atoms also has an important influence here, which in the case of metals (our case) plays the role of bond length. The greater the difference in sizes of atoms contained in the alloy, the more neighbors can be placed around an atom. Accordingly, the larger one atom is compared to the second, the more neighbors it will have, and, consequently, the fewer neighbors the atom with a smaller radius will have. Atomic radii: aluminum 143, nickel 124, cobalt 125, gadolinium 179, and terbium 180 pm. The radii of Gd and Tb atoms have the highest value, and each should have more than 12 atoms around it. In reality, as our research shows, gadolinium and terbium do not occupy positions in the center of icosahedra but rather act as catalysts for icosahedra formation. Figure 9 shows icosahedra in the supercooled melt at 500 K temperature, below T_g, for pressures of 0 and 10 GPa. Not all icosahedra were selected, but only nearly perfect ones, i.e., practically "ideal" ones with minimal deformations. As seen in Fig. 9, icosahedral clusters mainly include atoms of aluminum and gadolinium or aluminum and terbium, as well as a small number of nickel and cobalt atoms. As our calculations show, high pressure primarily affects the local environment of Gd, Tb, and Al in the melt. This is thermodynamically favorable for the formation of primary crystals of a new metastable phase Al_3(Gd/Tb), and a new phase Al(Gd/Tb) and a new phase $Al_8(Co/Ni)_4$(Gd/Tb) are formed. These metastable phases obtained under high pressure remain relatively stable for a long time under normal conditions.

The real experiment performed in this work and other studies [16, 18] has shown that multicomponent Al-TM-REM melts solidify into a series of non-trivial phases with different crystal lattices. When the system solidifies under high pressure, metastable phases are also synthesized. Today's numerical atomistic modeling can hardly reliably describe the solidification of a complex system of 4 or 5 elements into several coexisting non-trivial solid phases. However, it is possible to effectively model the melt with first-principles accuracy. Our numerical modeling of Al-TM-REM melts helped understand the role of impurities that cause the

formation of metastable phases during solidification. It is shown that REM alloying impurities act as catalysts for icosahedra formation in the melt. One impurity atom locally orders 12 atoms. The concentration of icosahedra in the melt is higher at high pressure. Thus, REM impurities increase the glass-forming ability of the system. It has been known for quite some time that alloys of the studied system form glass during rapid cooling of the melt (at a rate of 1,000,000 degrees/s) in the form of thin ribbons about 50 μm thick. We provided the first microscopic explanation for this by studying the melt, including under supercooling conditions. During slow cooling, the system does not vitrify but forms several coexisting solid phases with different crystal lattices. Probably, the high glass-forming ability of the alloys also indirectly affects this effect, as comparatively many completely dissimilar phases form. The emergence of such a multiphase disordered polycrystalline system is the result of high glassforming ability and frustration due to the presence of many icosahedra in the melt. It is known that the glass-forming ability of glass-forming phases (amorphizers) is due to their chemical nature and the presence of icosahedral coordination. They typically have a complex crystal lattice. The new primary phase emerging in the studied alloy $Al_3(Gd/Tb)$ can be considered as an alloy amorphizer. It is known that additional high-pressure treatment of the melt during rapid quenching can produce maximally "densified" – "ideal" glasses. We have shown the presence of a "percolation cluster" at high pressure in the studied metallic melt, which is usually a sign of glass-forming ability of melts. However, in the considered alloy under the selected production conditions, we did not detect an amorphous component. Apparently, for the amorphization of the studied melt, much higher pressures are needed at the same (considered) experimental cooling rate.

4. CONCLUSIONS

1. The experiment showed that during solidification of the melt $Al_{86}Ni_6Co_4Gd_2Tb_2$ with a temperature of 1800 K under pressure 7–10 GPa at a cooling rate of 1000 degrees/s, new crystalline metastable phases form in the alloy: a highly symmetric phase $Al_3(Gd/Tb)$ with a primitive cubic lattice ($cP4/2$), ordered by type Al_3U, containing Co and Ni and phase $Al_8Co_4(Gd/Tb)$ (type Al_8Cr_4Gd) with tetragonal structure($tI26/1$). The solid solution α-Al abnormally supersaturated with gadolinium and terbium. The sample structure is fine-crystalline with high density. The average microhardness is high due to solid solution and dispersion strengthening. At pressures less than 7 GPa, only equilibrium phases form in the alloy.

2. Through numerical modeling, the role of impurities in the alloy was determined, due to which metastable phases form. Alloying REM impurities are catalysts for the formation of icosahedral clusters in the melt. As pressure increases from 0 to 10 GPa, their quantity increases 8-fold, forming a "network" "percolation cluster," increasing the glass-forming ability of the melt. Using deep machine learning techniques, the dependence of glass transition temperatureT_g on high pressure was evaluated: pressure increase from 0 to 10 GPa raises T_g by 1.3 times.

The obtained results contribute to understanding the structure formation processes occurring in glass-forming melts of Al-TM-REM type in the eutectic region, as well as studying the effect of high pressure on their solidification processes. A deeper theoretical study of the system based on machine learning for constructing interatomic potential will allow considering much longer time intervals in numerical modeling and directly investigating solidification processes.

ACKNOWLEDGMENTS

The authors express gratitude to V. V. Brazhkin for his assistance in obtaining samples in the "toroid" type high-pressure chamber.

FUNDING

The work was carried out within the framework of the RSF Project (No. 22-22-00674). Electron microscopic studies were performed using the equipment of the Center for Physical and Physicochemical Methods of Analysis, Research of Properties and Characteristics of Surface, Nanostructures, Materials and Products at UdmFRC UB RAS, Izhevsk. Highpressure samples were obtained at IHPP RAS, Moscow, Troitsk. Numerical calculations were performed using the computing resources of the Federal Center for Collective Use Complex for Modeling

and Data Processing for Megascience Facilities of NRC Kurchatov Institute (http://ckp.nrcki.ru/), supercomputers of the Joint Supercomputer Center of RAS (JSCC RAS) and the Govorun supercomputer of the Multifunctional Information and Computing Complex LIIT JINR (Dubna).

REFERENCES

1. S. G. Rassolov, E. A. Sviridova, V. V. Maksimov et al., Metallofizika i Noveishie Tekhnologii 37, 1089 (2015).

2. A. L. Belyukov, S. G. Menshikova, and V. I. Ladyanov, J. Phys.: Cond. Matt. 35, 314001 (2023).

3. S. G. Menshikova, A. A. Sushkov, and V. V. Brazhkin, Phys. Sol. St. 64, 204 (2022).

4. N. M. Chtchelkatchev, M. V. Magnitskaya, V. A. Sidorov et al., Pure and Appl. Chem. 91, 941 (2019).

5. G. E. Abrosimova, A. S. Aronin, Phys. Solid State 59, 2227 (2017).

6. A. V. Tsvyashchenko, L. N. Fomicheva, A. A. Sorokin et al., Phys. Rev. B 65, 174513 (2002).

7. V. I. Levitas, J. Phys.: Cond. Matt. 30, 163001 (2018).

8. V. P. Filonenko, P. V. Zinin, I. P. Zibrov et al., Crystals 8, 448 (2018).

9. Yu. A. Sokolovskaya, V. V. Sokolovskiy, M.A. Zagrebin et al., JETP 125, 104 (2017).

10. A. M. Satanin, Introduction to the Density Functional Theory, Teaching aid., Nizhny Novgorod (2009), p. 64.

11. F. M. Gafarov, A. F. Galimyanov, Artificial Neural Networks and Applications, Kazan University Press, Kazan (2018).

12. E. O. Khazieva, N. M. Chtchelkatchev, A. O. Tipeev, R. E. Ryltsev, JETP 164, 980 (2023).

13. A. Yu. Churyumov, Cand. ... Dr. Tech. Sciences, Moscow (2008).

14. L. V. Kamaeva, E. N. Tsiok, and N. M. Chtchelkachev, J. Molec. Liquids 393, 123659 (2024).

15. L. N. Kolotova, G. E. Norman, and V. V. Pisarev, J. Non-Crystalline Sol. 429 (2015).

16. S. G. Menshikova, N. M. Chtchelkatchev, and V. V. Brazhkin, Materialia 28, 101713 (2023).

17. V. V. Brazhkin, Cand. ... Dr. phys.-mat. Sciences, Moscow (1996).

18. S. G. Menshikova and V. V. Brazhkin, Phys. Sol. St. 64, 197 (2022).

19. P. M. Larsen, S. Schmidt, and J. Schiotz, Modelling and Simul. in Mater. Sci. Eng. 24, 055007 (2016).

20. D. Turnbull, J. Appl. Phys. 21, 1022 (1950).

21. T. Schenk, D. Holland-Moritz, V. Simonet et al., Phys. Rev. Lett. 89, 075507 (2002).

22. T. V. Tropin, G. Schulz, J. W. Schmelzer et al., J. Non-Cryst. Solids 409, 63 (2015).

23. X. Guo, M. Potuzak, J.C. Mauro et al., J. Non-Cryst. Solids 357, 3230 (2011).

24. H. B. Ke, P. Wen, and W.H. Wang, AIP Adv. 2, 041404 (2012).

25. B. A. Rusanov, V. E. Sidorov, P. Svec et al., Inorganic Materials 56, 14 (2020).

26. T. V. Tropin, J. W. P. Schmelzer, and V. L. Aksenov, Physics-Uspekhi 59 (2016).